A Case Study of Ivory Species Identification Using a Combination of Morphological, Gemmological and Genetic Methods

Laurent E. Cartier, Michael S. Krzemnicki, Mario Gysi, Bertalan Lendvay and Nadja V. Morf

ABSTRACT: Twenty-one items sold as mammoth ivory in China were submitted to the Zurich Institute of Forensic Medicine (University of Zurich, Switzerland) and SSEF for testing. The aim of this case study was to identify these samples using macroscopic morphological diagnostics, microscopic examination, FTIR spectroscopy, trace-element analysis and additional minimally destructive DNA analysis (of approximately 100 mg of powder) of a region of the cytochrome *b* gene to assign taxonomic identification. Morphological features (Schreger angles) shown by five of the samples were characteristic of extinct Proboscideans (mammoths), and one other specimen displayed unnatural layering that identified it as an ivory imitation. FTIR spectroscopy further showed the imitation was an artificial resin, while infrared spectra of the other samples displayed overlapping features characteristic of carbonated hydroxyapatite (i.e. ivory or bone). Like FTIR spectroscopy, trace-element chemistry cannot be used to separate species. DNA analysis could in some cases differentiate extinct (mammoth) from extant (African and Asian elephant) Proboscidean species, and also identified one specimen as cattle bone. Combining morphological, gemmological and genetic approaches can increase the amount of evidence available to identify the species origin of ivory.

The Journal of Gemmology, **37**(3), 2020, pp. 282–297, https://doi.org/10.15506/JoG.2020.37.3.282

Ivory (e.g. Figure 1), a mammalian tooth or tusk of commercial interest, has been valued since ancient times (Espinoza & Mann 2000). Ivory is produced by a large number of animal taxa (e.g. walrus, warthog and whale), among which elephant ivory is the most studied due to its value, popularity and cultural importance (Campbell Pedersen 2015). African (*Loxodonta* spp.) and Asian (*Elephas maximus*) elephants, along with their extinct relatives (e.g. mammoths, *Mammuthus* spp.), belong to the mammalian taxonomic order Proboscidea. These taxa produce ivory that is made up of collagen and carbonated hydroxyapatite (Edwards *et al.* 2006), which can be finely carved and is therefore sought after.

Among the extinct Proboscidea species, only the ivory of the woolly mammoth (*Mammuthus primigenius*) is suitable for carvings and jewellery use, as this is the only species with tusks that have been well preserved since the end of the Pleistocene (10,000–11,000 years ago) in high-latitude permafrost areas (Nikolskiy *et al.* 2011). Ivory from *Mammuthus primigenius* is abundant in certain parts of Siberia and Alaska, and mammoth ivory has appeared more widely on the market in recent years (Vigne & Martin 2014), as restrictions on the international trade of elephant ivory have taken force (e.g. under the Convention on International Trade in Endangered Species of Wild Fauna and Flora, or CITES; www.cites.org/eng/niaps).

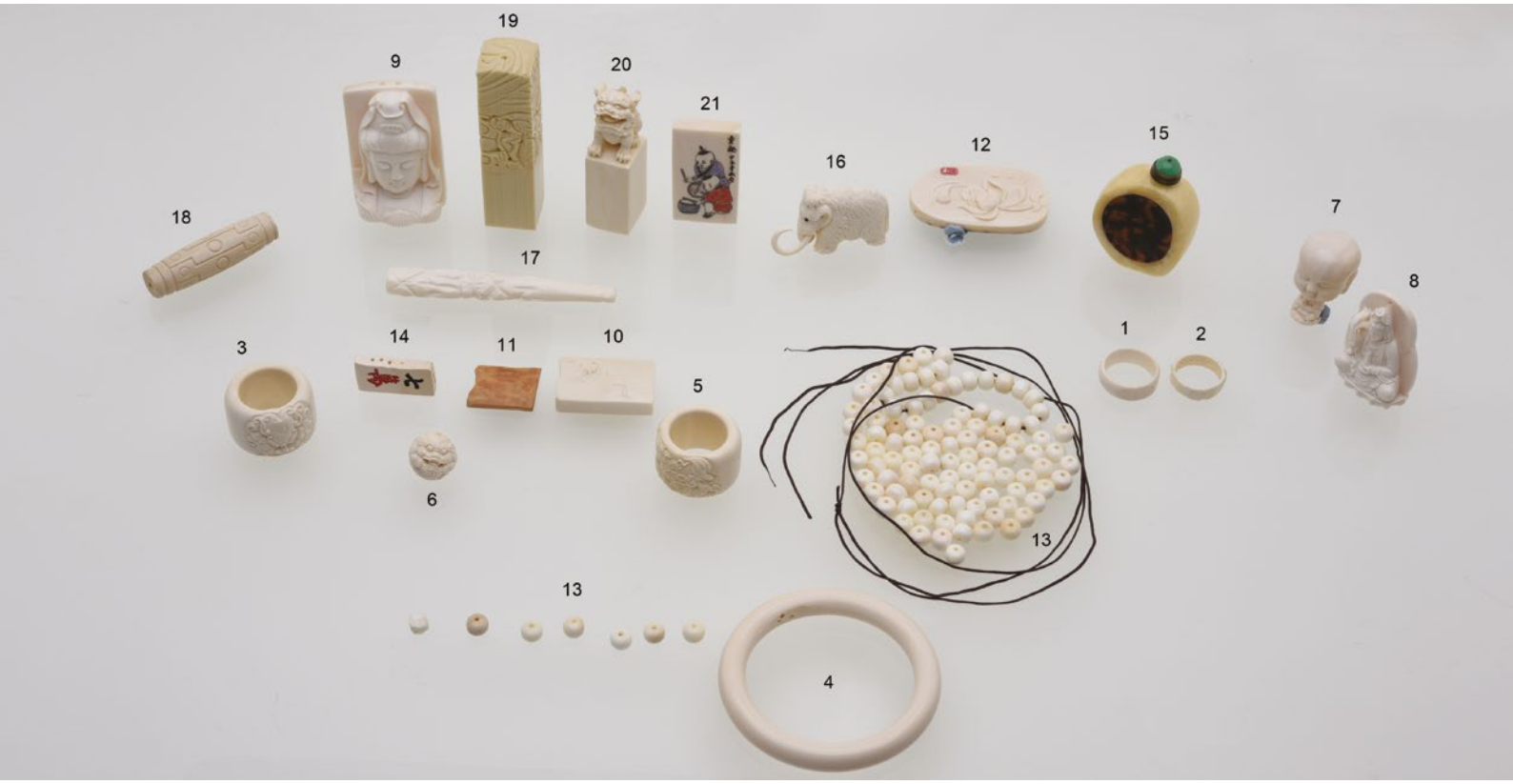

Figure 1: The 21 specimens submitted for testing (including a strand of 108 beads that are grouped together as sample no. 13) were purchased in China, where they were represented as 'mammoth ivory'. See Table I for sample weights. Photo by Vito Lanzafame, SSEF.

Given the regulations on elephant ivory, and the free trade in mammoth ivory, it is necessary to develop and apply scientific methods that can assign an ivory sample to its correct taxonomic species.

This article presents a case study exploring a range of methods used collectively to identify the species of 21 samples that were sold on the Chinese market as mammoth ivory. Our examination included morphological evaluation based on Schreger angles, Fourier-transform infrared (FTIR) spectroscopy and trace-element analysis of six selected specimens. When morphological assessment of the species was not possible, we performed DNA analysis.

BACKGROUND

Currently, the identification of elephant and mammoth ivories, and their distinction from other forms of ivory or imitations, rests largely on macroscopic morphological observation, although it can be supplemented by DNA analysis depending on the context. Morphological identification was outlined by Espinoza & Mann (2000) in a document that is widely used by customs agents and wildlife forensic scientists worldwide; this reference guide was updated in August 2020 (Baker *et al*. 2020). The main criterion to identify ivory is the presence of Schreger lines, which are present only in Proboscidean material. The angle formed by the Schreger lines can be used to differentiate between extant (recently living) African and Asian elephants, and extinct Proboscidea (mammoths), as explained below. However, Schreger lines are often not visible enough on processed (carved and polished) samples to make a conclusive identification.

Ivory has been studied using techniques such as Raman and Fourier-transform infrared spectroscopy (Edwards & Farwell 1995; Shimoyama *et al.* 2004; Edwards *et al.* 2006), along with detailed visual analysis and trace-element studies (Singh *et al.* 2006; Yin *et al.* 2013). However, as outlined by the United Nations in its *Guidelines on Methods and Procedures for Ivory Sampling and Laboratory Analysis* (UNODC 2014), FTIR and Raman spectroscopy can be employed to distinguish genuine carbonated hydroxyapatite-based ivory from ivory imitations such as resin, but FTIR spectroscopy should not be used to determine the animal species. Therefore, UNODC (2014) recommends that morphological and genetic methods be used for the forensic species identification of ivory.

Table I: Results of the morphological analysis of the 21 samples.

Sample no.	Item	Weight (ct)	Schreger lines visible?	CDJ[a] visible?	Schreger angle[b] (average and min.–max.)	Taxonomic identification[c]
1	Ring, carved	6.71	Yes	No	—	Proboscidea
2	Ring, carved	4.33	Yes	No	—	Proboscidea
3	Ring, carved	71.59	Yes	No	—	Proboscidea
4	Bangle	117.42	Yes	No	—	Proboscidea
5	Ring, carved	63.42	Yes	No	—	Proboscidea
6	Bead, carved	19.50	Yes	No	—	Proboscidea
7	Head and stand, carved	74.81	Yes	Yes (head)	83.2° (77°–87°)	Extinct Proboscidea
8	Plaque, carved	70.98	Yes	No	—	Proboscidea
9	Plaque, carved	211.13	Yes	Yes	94.2° (91°–99°)	Extinct Proboscidea
10	Plaque, carved	52.21	Yes	No	—	Proboscidea
11	Slab	10.36	No	No	—	Not possible
12	Plaque, carved	109.20	Yes	Yes	72.6° (53°–86°)	Extinct Proboscidea
13	Beads (108), drilled	~1.2 each	Yes	Yes (seven beads)	Two beads: 72.6° (70°–75°), 84.5° (82°–88°)	Extinct Proboscidea
14	Plaque, polished	17.91	Yes	No	—	Proboscidea
15	Snuff bottle	150.53	No	No	—	Not possible
16	Mammoth, carved	70.27	Yes	Yes (tusks)	Not possible (too small)	Proboscidea
17	Pipe mouthpiece, carved	47.62	No	No	—	Not possible
18	Bead, carved	59.46	Yes	No	—	Proboscidea
19	Stamp, carved	247.02	No	No	—	Ivory imitation
20	Stamp, carved	151.59	No	No	—	Not possible
21	Block, painted	82.78	Yes	Yes	82.2° (77°–86°)	Extinct Proboscidea

[a] CDJ = cementum-dentine junction.
[b] Schreger angles are provided only for samples on which the CDJ was visible.
[c] The standalone term 'Proboscidea' indicates that it was not possible to differentiate whether a specimen consisted of extant or extinct Proboscidean ivory.

Various genetic methods have been developed and used to identify species of Proboscidean ivory (Gupta *et al.* 2011; Wozney & Wilson 2012; Lee *et al.* 2013; Kitpipit *et al.* 2016, 2017; Conte *et al.* 2019; Ngatia *et al.* 2019). However, among these studies, only Lee *et al.* (2013) used the so-called *DNA barcoding* methodology—that is, using a specific and targeted genome region, which allows identification of both extinct and extant Proboscidean species, as well as the species of other types of ivory or ivory imitations (e.g. bone). All other previously applied techniques simply give a negative result (i.e. not Proboscidean ivory) if the ivory item originated from taxa other than those specifically targeted by the assay. Applying DNA barcoding methodology using universal primers[1] can be less sensitive than a species-specific assay, but it can provide additional information about a tested item, as it allows for the identification of a broad array of species. Such markers show variations between species, but are generally invariable within species; this makes them ideal for differentiating species

[1] For definitions of some terminology related to genetic testing, see the glossary on p. 157 of Cartier *et al.* (2018).

based on DNA (Tobe & Linacre 2010). Nevertheless, analysing these markers (based on Sanger sequencing) is not possible if a sample contains a mixture of DNA from different species. This is often the case when a specimen is very old and/or has little DNA (such as ivory from extinct Proboscideans), for which various contaminants (e.g. bacterial DNA, polishing residues or human DNA) can make up significant portions of the total DNA. To help deconvolute such species mixtures, a technique called *massive parallel sequencing* can be used (Budowle *et al.* 2016).

Although not employed in this study, isotopic analysis of ivory samples (van der Merwe *et al.* 1990; Ziegler *et al.* 2016) has been applied as an investigative technique to combat elephant poaching by further narrowing the geographic source region of an ivory sample. Another test—also beyond the scope of this article—to determine whether unknown specimens are from extinct or extant Proboscideans is age dating (e.g. carbon-14). This technique has been used to determine the age of seized elephant ivory (Schmied *et al.* 2012; Cerling *et al.* 2016), and has also been applied to mammoth samples (Basilyan *et al.* 2011), and could thus be useful to distinguish recent elephant ivory from extinct mammoth ivory. Furthermore, radiocarbon age dating can determine whether or not an elephant lived before or after the atomic 'bomb peak' (around 1950), and can thus be used to determine whether ivory should be classified as pre-CITES material (i.e. before 1 July 1975 for the Asian elephant and before 26 February 1976 for the African elephant; Brunnermeier *et al.* 2012; Schmied *et al.* 2012). Importantly, these dates and laws are not the same in every country; some are stricter or date further back than CITES regulations. For example, the UK has banned the sale of elephant ivory worked after 1947 (Harris *et al.* 2019).

MATERIALS AND METHODS

Twenty-one specimens (including multiple beads sold as a strand and classified as one sample; Figure 1 and Table I) were purchased as mammoth ivory from different dealers and shops in China and submitted to the Zurich Institute of Forensic Medicine and SSEF for testing.

Morphological Analysis Using Schreger Angles

The Schreger pattern was first described by Bernard Schreger (1800), and consists of sets of intersecting lines that radiate in a spiral fashion from the axis of a tusk (Trapani & Fisher 2003), as for example in Figure 2. According to Trapani and Fisher (2003, p. 429), 'light and dark regions forming these lines are thought to be macroscopic manifestations of systematic shifts in undulatory pathways of dentinal tubules, produced by odontoblasts as they move towards the tusk axis during dentin [*sic*] deposition'. The Schreger angle is the angle at which dextral and sinistral Schreger lines intersect. Outer Schreger angles (i.e. those closest to the outside of the tusk) are acute in extinct Proboscideans (i.e. mammoths) and obtuse in extant Proboscideans (i.e. elephants; Espinoza & Mann 1993, 2000). Mammoth ivory samples examined by Espinoza & Mann (2000) consistently showed outer Schreger angles that averaged below 100° (typically 73°), whereas the tested elephant specimens exhibited angles with averages above 100° (typically 124°). For samples with angles falling in the range of 90°–110°, it is important that multiple angle measurements be carried out and averaged (Espinoza & Mann 2000).

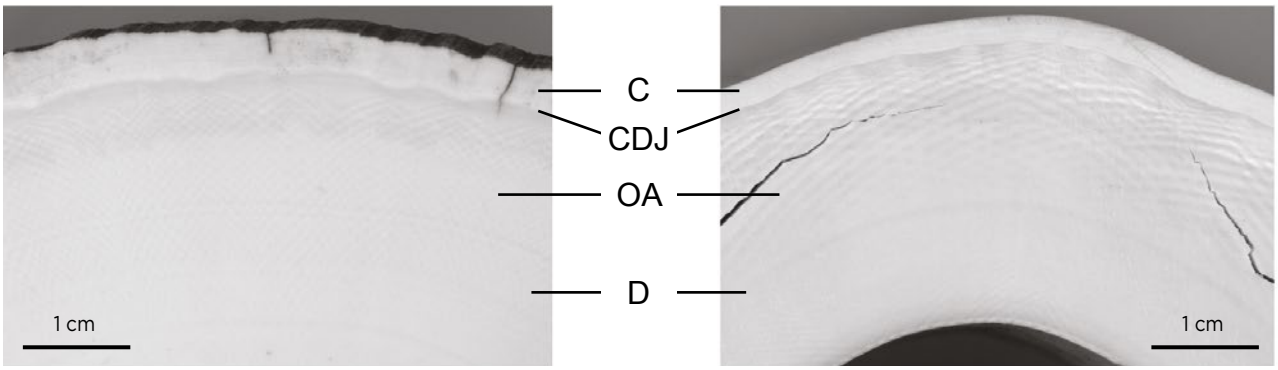

Figure 2: The angles formed by Schreger lines are shown here in extinct (left) and extant (right) Proboscidean ivory cross-sections. The outer Schreger angles (OA) in the dentine (D) closest to the cementum (C) show diagnostic differences. The cementum-dentine junction (CDJ) must be present in a sample for Schreger angles to be used reliably. Photos by Ed Espinoza.

The cementum (a layer of mineralised dental tissue which covers the outside of the tusk) must be visible for the correct reading of Schreger angles, in order to orient the sample within the tusk. Unfortunately, the cementum-dentine junction (CDJ) is not always present in worked specimens. Because only the outer Schreger lines can be used for diagnostic angle measurement, it is vital to orient a sample based on the presence of the CDJ. Research by Trapani and Fisher (2003) on specimens with and without cementum confirmed that if a sample cannot be oriented, and if the Schreger angles are measured from inner lines, then misidentifications can occur.

All 21 specimens in this study were subjected to meticulous microscopic and morphological characterisation, but only six of them were found to contain the CDJ and were therefore potentially useful for Schreger angle measurements.

Infrared and Chemical Analysis

All 21 samples were investigated by infrared spectroscopy at the Swiss Gemmological Institute SSEF using a Nicolet 550 FTIR spectrometer in transmission mode with the KBr pellet method (Khoshhesab 2012). An average of 0.5 mg of powdered material was taken from each ivory sample for each measurement. Spectra were collected in the range of 6000–400 cm^{-1} with a resolution of 0.5 cm^{-1} and 32 scans per spectrum at room temperature (25°C).

Trace-element chemistry cannot be used to clearly separate ivory species (more research and a larger data set are needed), and is thus provided here to contribute to the further chemical characterisation of ivory samples in general. Laser ablation inductively coupled plasma time-of-flight mass spectrometry (LA-ICP-TOF-MS) was used to determine the trace-element composition of six selected specimens (nos. 10, 11, 14, 16, 17 and 21). These were considered to be representative of the sample lot, and also nos. 11 and 17 could not be conclusively identified using other techniques and were thus selected for trace-element characterisation to obtain additional data. The analyses were performed at SSEF using a 193 nm ArF excimer laser (ESI/New Wave Research NWR193UC) coupled to a commercial ICP-TOF-MS unit (Tofwerk icpTOF) with helium as the carrier gas. A detailed description of this method and set-up can be found in Wang *et al.* (2016). TOF-MS allows simultaneous analysis of the full range of masses (from ^{7}Li to ^{238}U), so no preselection of elements (isotopes) of interest was necessary. To calculate element concentrations, we used NIST610 glass as an external standard and the stoichiometry of Ca in hydroxyapatite as an internal standard. Although not matrix-matched, this approach using NIST glass standards has been applied in numerous previous studies on biogenic calcium carbonates and phosphates (Lee *et al.* 1999; Cucina *et al.* 2007; Limbeck *et al.* 2015; and references therein). Each sample was measured at two different locations using an ablation spot size of 75 µm and 20 Hz ablation frequency.

Genetic Analysis

Genetic analysis was performed on 16 samples (i.e. those for which morphological analysis was not possible) at the Zurich Institute of Forensic Medicine, University of Zurich, Switzerland. The method for DNA extraction and the polymerase chain reaction (PCR) set-up selected to analyse the ivory specimens were standardised and validated in the ISO 17025 accredited laboratory facilities where this work was carried out. Although this methodology may not be typical for identifying Proboscidean ivory, it allows species identification also for non-Proboscidean samples.

Prior to DNA extraction, the samples were cleaned with Dr. Weigert 5% neodisher LM 3 detergent and rinsed with deionised water and 70% ethanol. About 100 mg of ivory powder were acquired from each specimen by drilling a small hole on the back or base of the sample. We used a Proxxon Micromot 50 (E) drill with a 4–6 mm diameter cone-shaped grinding bit, taking care to avoid heating up the specimen by not pressing hard and including regular pauses to let the drill head cool down. To avoid contamination, the powder produced from the initial external surface was discarded. The size and shape of some samples, and especially the desire to not alter the item's appearance, made the cleaning and drilling process very challenging.

DNA was isolated from the powdered ivory samples using a Thermo Fisher Scientific PrepFiler BTA Forensic DNA Extraction Kit, following the manufacturer's protocol for the extraction of DNA from calcified tissues (bone or tooth). For species identification, a region of the cytochrome *b* gene was amplified as described by Morf *et al.* (2013). A Beckman Coulter AMPure XP bead system was used to purify the PCR products, which were then quantified with a Thermo Fisher Scientific Qubit 4 fluorometer. To explore the utility of the massive parallel sequencing technique for performing species identification, sequencing libraries were constructed with the Thermo Fisher Scientific Ion Plus Fragment Library Kit and Ion Xpress barcode adapters, beginning with the end repair of the purified PCR products. End repair and all subsequent steps of the manufacturer's protocol were conducted by reducing all reaction volumes to one quarter and using 2.4 ng DNA input if possible.

The barcoded libraries were then quantified with a Thermo Fisher Scientific Ion Library TaqMan Quantitation Kit, and all samples were pooled with equimolar concentrations. The 26 micromolar pooled libraries were used for templating on a Thermo Fisher Scientific Ion OneTouch 2 System. Sequencing was carried out on a Thermo Fisher Scientific Ion PGM platform. Adapter-trimmed sequence data were exported to FASTQ files using the FileExporter Plugin within Torrent Suite 5.10 software. The sequences were quality filtered using USEARCH (Edgar & Flyvbjerg 2015) and clustered into operational taxonomic units (OTUs) with UPARSE (Edgar 2013) at 97% minimal identity threshold (default setting; other values were tested but did not make significant differences) and a minimal OTU size of 100 sequence reads (to analyse major components and exclude noise sequences).

The resulting sequences of the OTUs were then compared to DNA sequences stored in the online GenBank database of the National Center for Biotechnology Information (NCBI; Bethesda, Maryland, USA). We identified DNA sequence entries of the GenBank database that were most similar to the DNA sequences obtained from our samples by searching the database with the MegaBLAST function of NCBI. That way, each OTU was assigned to a taxonomic rank; ideally an OTU would correspond to a species. For each sample, read numbers pertaining to different taxonomic ranks were expressed as a percentage of the entire sequence read number. Sequences belonging to the domain of bacteria and OTUs that could not be identified via the MegaBLAST function were grouped together into one category. To exclude rare contaminants, taxonomic ranks below 10% of the total read number were not considered during evaluation of the sample. To see the relationship of the ivory DNA sequences of this study to those of extant Proboscideans and *Mammuthus primigenius*, a Bayesian phylogenetic tree was constructed using MrBayes version 3.2.7 software (Ronquist *et al.* 2012), as described by Lendvay *et al.* (2020). As reference data, we used five homologous DNA sequences of each extant Proboscidean species and *Mammuthus primigenius*, respectively. Furthermore, DNA sequences of the closely related rock hyrax (*Procavia capensis*) and dugong (*Dugong dugon*) were included as outgroup taxa. All reference data were downloaded from the GenBank database.

RESULTS AND DISCUSSION

Morphological Analysis

Schreger angles were successfully measured on five of the samples (with one sample [no. 5] consisting of two beads; see Table I). Figure 3 illustrates the location of the CDJ in one of these specimens, which is a prerequisite for morphological identification based on Schreger angles. The range of average measurements obtained from the five samples was 72.6°–94.2°. All of these measurement averages are below 100°, which according to Espinoza & Mann (2000) corresponds to the suggested limit to separate elephant ivory (above 100° average) from mammoth ivory (below 100° average). These five samples were thus conclusively identified as ivory originating from extinct Proboscideans. Therefore, further DNA analysis was not deemed necessary and was thus not carried out on those specimens.

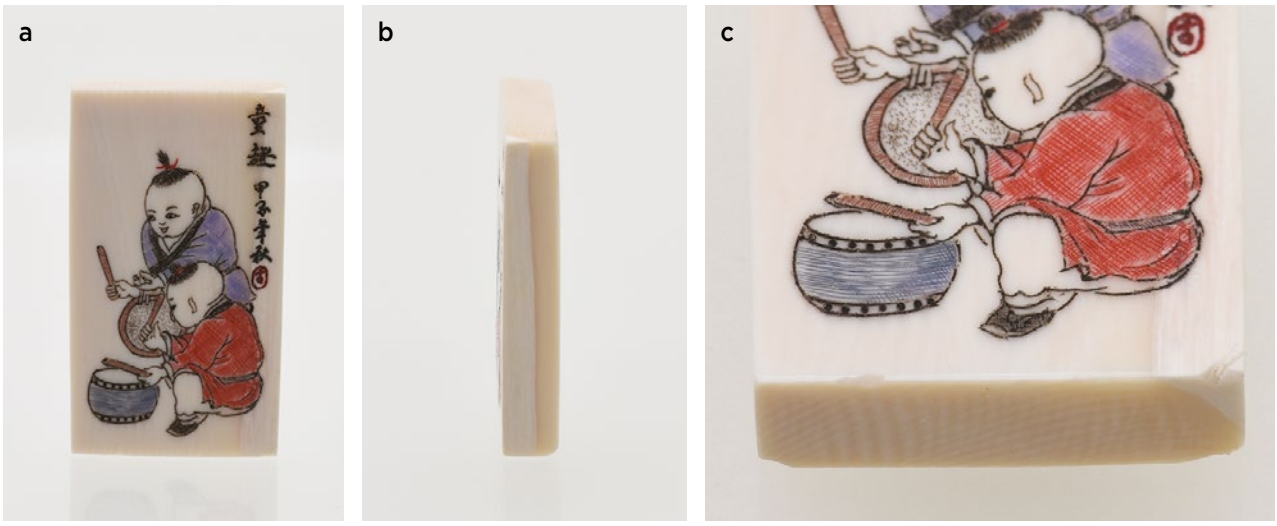

Figure 3: Sample 21 is a carved block of ivory (about 4 cm tall) that is decorated by a painting (**a**). Views of the side (**b**) and base (**c**) clearly show the cementum-dentine junction. The white part to the left in the side view is cementum, whereas the beige material on the right side is dentine. Image (c) shows cementum (white) at the upper right, next to the outer Schreger lines. The Schreger angle of these lines averaged 82.2°, which is characteristic of mammoth ivory. Photos by Vito Lanzafame, SSEF.

Although Schreger lines were observed in 11 other samples, their intersection angle could not be used due to orientation issues (absence of visible CDJ). Nevertheless, based only on the presence of the Schreger lines, these specimens could be identified as being Proboscidean.

The remaining five samples showed no Schreger lines, and no. 19 was visually identified as an ivory imitation based on the presence of a distinct layered structure intended to simulate the Schreger lines of ivory.

FTIR SPECTROSCOPY

All samples except for the ivory imitation showed FTIR spectral characteristics of carbonated hydroxyapatite (Figures 4 and 5; cf. Chang & Tanaka 2002; Grunenwald *et al.* 2014; Chappard *et al.* 2016). Figure 4 highlights a particular case (ivory bangle sample no. 4) where Schreger lines were visible but not conclusive for species identification (due to the absence of the CDJ). By contrast, specimen no. 19 yielded a very different FTIR spectrum dominated by sharp peaks (Figure 6) and was readily identified as an ivory imitation made of artificial resin (by comparison to the Thermo Scientific spectral library). The FTIR spectrum of sample no. 17 (see Figure 5) showed a characteristic carbonated hydroxyapatite spectrum, suggesting that it is of dentine or bone origin, but it could not be attributed to a specific species or species group with the methods used.

As (mammoth) ivory ages over time, carbonated hydroxyapatite can recrystallise. Furthermore, as weathering occurs, amide/phosphate ratios and carbonate/phosphate ratios can change (Jacob *et al.* 2008). Multiple factors can influence an FTIR spectrum (age, weathering state, crystallinity, collagen content and location of the sample in a tusk), so FTIR spectroscopy is not a reliable method to determine the species of ivory (see also UNODC 2014). This case study—and further unpublished research by the authors on elephant ivory from the SSEF reference collection—confirm this fact, as we could not identify clear distinguishing factors to separate elephant ivory from fossilised mammoth ivory based on FTIR spectral features.

This result is, however, different from that of Yin *et al.* (2013), who suggested a possible separation of modern elephant ivory from mammoth ivory based on FTIR spectroscopy, mainly by attributing observed differences in the spectra to the burial of mammoth ivory and related loss of water and degradation of collagen. Although such weathering-related processes are possible, their influence on FTIR spectra remains unclear (O'Connor *et al.* 2011). Our FTIR spectra of both modern elephant ivory and extinct (buried) mammoth ivory samples from the SSEF reference collection did not reveal any notable or conclusive difference in the hydroxyl range (3500–2900 cm^{-1}) or in the CH⁻ range (3000–2800 cm^{-1}). Based on our analyses, we thus presume that the spiky 'peaks' in the 3500–2900 cm^{-1} range of the FTIR spectra reported by Yin *et al.*

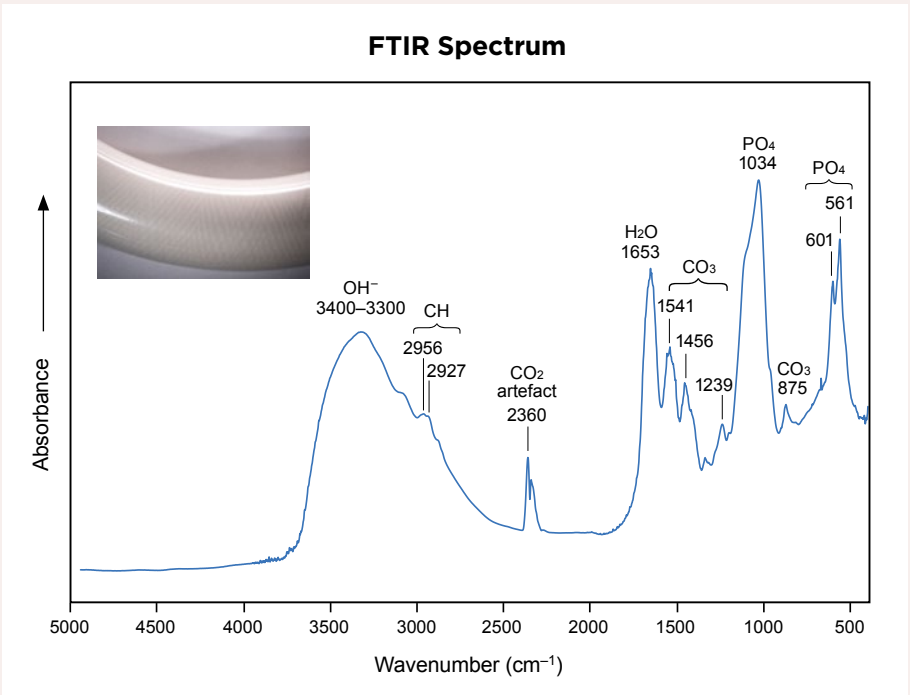

Figure 4: The FTIR spectrum of sample no. 4 (mammoth ivory bangle) shows absorption bands characteristic of carbonated hydroxyapatite (e.g. ivory and bone) and collagen. Peak attributions are after Hassan *et al.* (2016) and the artefact at 2360 cm^{-1} is from atmospheric CO_2. The inset shows Schreger lines in the bangle (which is approximately 1 cm thick; photo courtesy of SSEF), but the absence of the CDJ precludes identification based on Schreger angles.

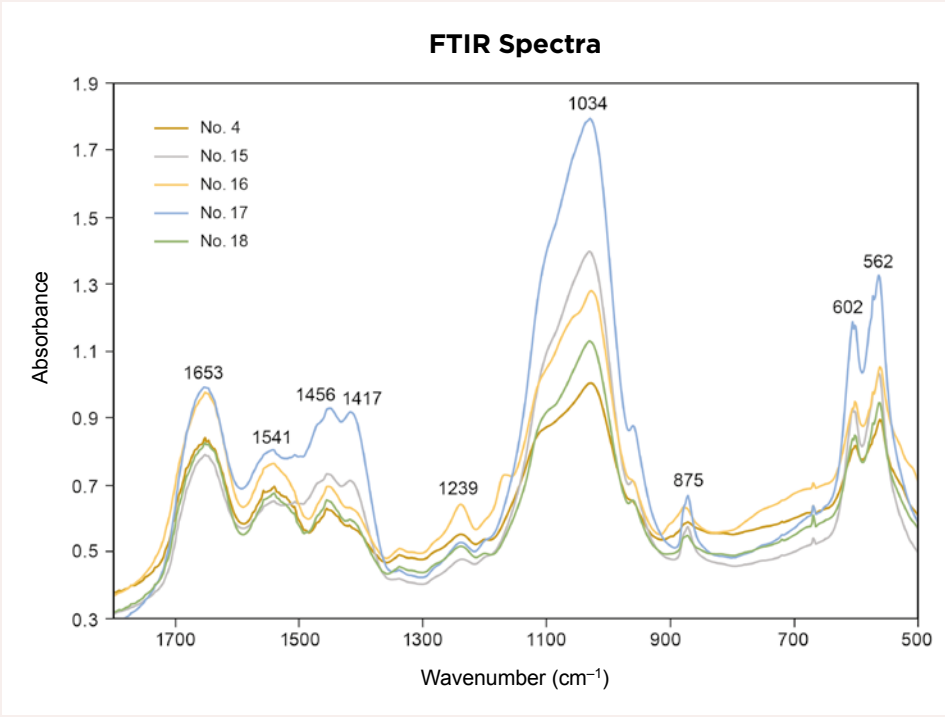

Figure 5: FTIR spectra (in the 1800–500 cm^{-1} range) of mammoth ivory (nos. 4 and 16) and undifferentiated Proboscidea (no. 18) are compared to cattle bone (no. 15, identified using DNA analysis) and one unidentified sample (no. 17). Regardless of their taxa, all these specimens show very similar spectral features characteristic of carbonated hydroxyapatite.

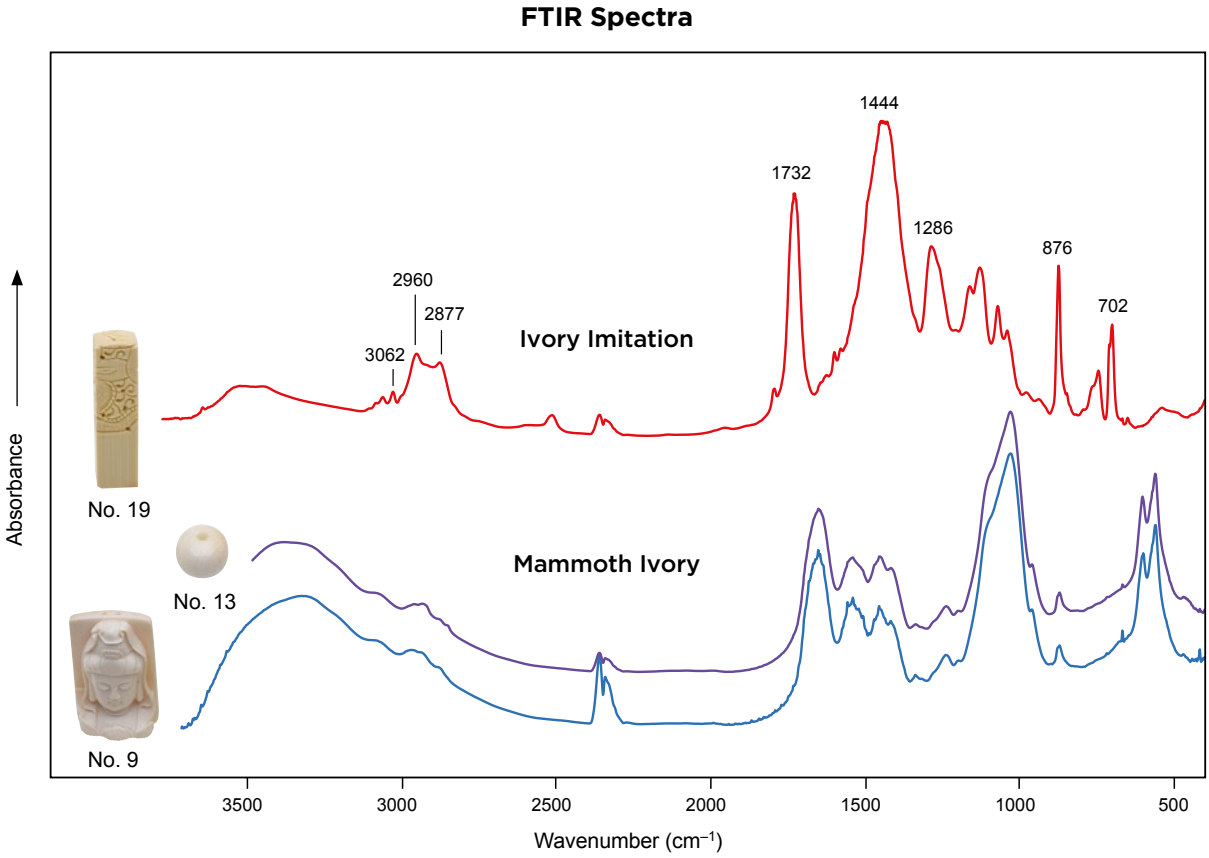

Figure 6: The FTIR spectrum of an ivory imitation (artificial resin, no. 19) is dominated by sharp polymer-related bands, and is compared to two samples of mammoth ivory (nos. 9 and 13) that display characteristic features of carbonated hydroxyapatite. Inset photos by Vito Lanzafame, SSEF; the specimens are 3.5 cm wide (no. 9), about 0.5 cm in diameter (no. 13) and 7 cm tall (no. 19).

(2013)—which were described by them as a result of water loss—are in fact artefacts due to total absorption in the hydroxyl range of their mammoth sample. In any case, the present study clearly reveals that species identification or age estimation (modern vs. fossil) of ivory based on FTIR spectroscopy is not reliable.

Trace-Element Analysis

Polycrystalline hydroxyapatite can accommodate a broad range of trace elements, primarily as substitutions for the large Ca^{2+} cation (Brown & Constantz 1994). A selection of relevant elements is listed in Table II for the six samples analysed by LA-ICP-TOF-MS. A comparison of our data to the literature (Kohn *et al.* 1999 and references therein) reveals high consistency with reported concentration ranges for fossil dentine. Each specimen was analysed on two randomly selected areas, and our data suggest that each one was very homogeneous in its trace-element concentrations. Interestingly, three of the samples (nos. 14, 16 and 21, all identified as extinct Proboscidea by their morphology or DNA testing, as covered below) showed distinctly higher Mg but lower concentrations of Fe, Sr and Ba compared to sample no. 10 (undifferentiated Proboscidea). Specimen no. 11 (which could not be identified) was characterised by relatively high Mn, Fe and, to some extent, Sr, Ba and rare-earth elements (REEs). This might be related to alteration during burial in soil (diagenesis), as this sample looked weathered and was reddish brown (Figure 7), as if stained by Fe-Mn (hydr)oxides. Specimen no. 17 (also not identifiable) differed in having higher Na, Zn, Ba and REEs compared to the other samples.

Genetic Analysis Based on a Region of the Cytochrome b Gene

DNA analysis was carried out on 16 of the 21 samples, and was successful for 15 of them. For one specimen (no. 11), no PCR product could be amplified, most likely

Table II: LA-ICP-TOF-MS trace-element data (in ppmw) for six selected samples.[a]

Sample no.	Spot	B	Na	Mg	Si	Cr	Mn	Fe	Zn	Sr	Ba	REE	Pb	U/Pb	Taxonomic identification (based on morphology or DNA)
10	1	7.85	4415	7653	266.3	1.186	153.9	639.2	34.17	994.3	95.28	0.208	0.153	0.10	Proboscidea
	2	7.45	4372	7381	265.7	1.054	147.6	614.4	36.62	971.9	92.89	0.193	0.166	0.12	
11	1	5.46	2700	1470	343.8	0.539	4808	26300	38.89	1315	768.8	1.236	0.061	0.30	Not possible
	2	5.90	2770	1468	321.6	1.132	4758	26260	40.24	1311	767.9	1.228	0.054	0.21	
14	1	8.28	3081	43370	339.3	1.124	0.899	31.69	25.81	318.3	48.16	0.125	0.108	0.12	Extinct Proboscidea
	2	7.61	3172	37830	281.7	0.902	0.850	24.41	27.36	316.9	46.74	0.083	0.180	0.10	
16	1	14.07	4172	42690	255.7	1.150	0.924	28.55	34.92	385.8	15.52	0.021	0.030	na	Extinct Proboscidea
	2	14.02	4297	41460	288.3	0.790	0.913	25.07	34.79	386.1	15.67	0.045	0.031	0.19	
17	1	5.95	8423	5554	218.4	0.653	0.931	26.94	121.9	609.4	719.7	1.112	0.633	0.01	Not possible
	2	6.05	8262	5467	199.4	0.451	1.164	25.47	136.8	599.7	752.9	1.221	0.755	na	
21	1	11.19	4905	39250	292.6	0.908	0.948	20.11	28.22	345.6	45.47	0.130	0.185	0.08	Extinct Proboscidea
	2	11.83	5205	36220	314.6	0.782	0.971	22.42	31.52	356.1	44.50	0.142	0.200	0.15	
Reference values (Kohn *et al.* 1999)		>10–10s	1000s	1000s	10–~100s	nr	nr	nr	100s–1000s	100s–~100	10s–~100	<1	nr	<1	Fossil dentine[b]

[a] Abbreviations: na = not applicable because U was below the detection limit; nr = not reported by Kohn *et al.* (1999).
[b] Range of values from Burchell's zebra (*Equus burchellii*), Guenther's dik-dik (*Rhynchotragus guentheri*) and Grant's gazelle (*Gazella granti*).

Figure 7: This weathered sample (no. 11; about 2 cm wide) was found to contain relatively high Fe and Mn concentrations. Its colour and chemistry might be related to alteration during burial in soil, resulting in impregnation with Fe-Mn (hydr)-oxides. Photo by V. Lanzafame, SSEF.

due to too little or too degraded DNA. By using massive parallel sequencing to analyse the genetic data, we were able to deconvolute mixtures and infer the different DNA contents of a specimen. Detected bacterial species were excluded as a possible origin. Any human DNA detected as a minor component in a mixture was considered a contaminant and was not included in the final taxonomic identification.

The taxonomic origin of nine samples was identified as extinct Proboscidea, one specimen originated from the genus *Bos* (wild and domestic cattle) and the DNA analysed for another sample was of human origin (Table III). The DNA extracts of the remaining four specimens were identified as DNA mixtures in which human DNA accounted for the largest part. The minor parts of these mixtures originated from the following taxonomic ranks: *Mammuthus* sp. (mammoths), *Loxodonta* sp. (African elephants), *Gallus gallus* (junglefowl, e.g. chickens) and bacteria.

Table III: Results for 16 samples based on DNA analysis, including total number of sequence reads per sample.*

Sample no.	Total no. of reads	*Mammuthus* sp.	*Homo sapiens*	*Loxodonta* sp.	*Bos* sp.	*Gallus gallus*	Bacterial or unidentifiable sequences	Sequences below threshold	Taxonomic identification
1	1012	70.7	14.7					14.7	Extinct Proboscidea
2	6850		73.1	13.2			13.3	0.3	Mixture
3	17855	98.8						1.2	Extinct Proboscidea
4	20580	98.5						1.5	Extinct Proboscidea
5	20285	98.5						1.5	Extinct Proboscidea
6	12070	95.3						4.7	Extinct Proboscidea
8	3251	30.2	66.7					3.1	Mixture
10	996		62.3			37.3		0.4	Mixture
11									Not possible
13	2939	99.5						0.5	Extinct Proboscidea
14	13931	73.9	21.3					4.8	Extinct Proboscidea
15	6317				62.9		33.2	3.9	*Bos* sp.
16	10958	56.7	41.8					1.6	Extinct Proboscidea
17	5974		81.5			12.0		6.6	Mixture
18	10833		93.1					6.9	*Homo sapiens*
20	14908	97.8						2.2	Extinct Proboscidea

* The read numbers pertaining to different taxonomic ranks are expressed as percentages of the entire sequence read number, and sequences of OTUs with less than 100 reads are grouped together with sequences of taxonomic ranks with less than 10% of the total read number in the category titled 'Sequences below threshold'.

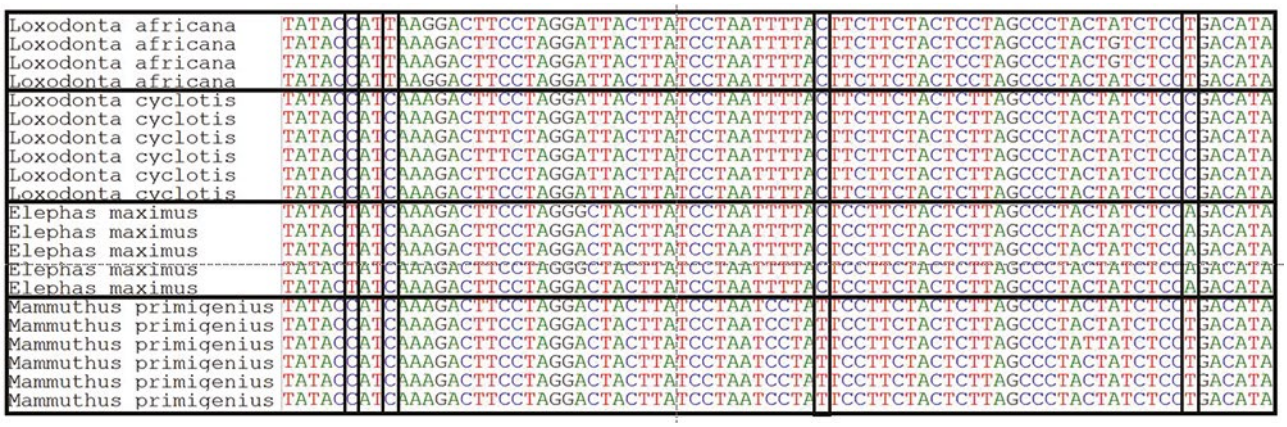

Figure 8: Nucleotide differences between extant Proboscidean species and the woolly mammoth (*Mammuthus primigenius*) are bracketed by vertical lines in this DNA sequence alignment of a short fragment of the mitochondrial cytochrome *b* gene.

Separating Mammoth and Elephant Ivory Using Genetic Analysis

To demonstrate how our genetic analysis is able to differentiate between elephant and mammoth ivory, we compared sequences from different Proboscideans in the online NCBI database. Figure 8 shows examples of nucleotide (A, C, G, T) differences between the extant Proboscidean species and the woolly mammoth (*Mammuthus primigenius*) in a short fragment (length: 78 base pairs) of the mitochondrial cytochrome *b* gene. The sequences of the extinct Proboscidea (length: 359 base pairs) obtained in this study showed 10 or more nucleotide differences from the sequences of African or Asian elephants found in the NCBI database.

These sequences from the extinct Proboscidean samples were included in a Bayesian phylogenetic tree containing sequences of extant Proboscideans and *Mammuthus primigenius* (Figure 9). A phylogenetic tree

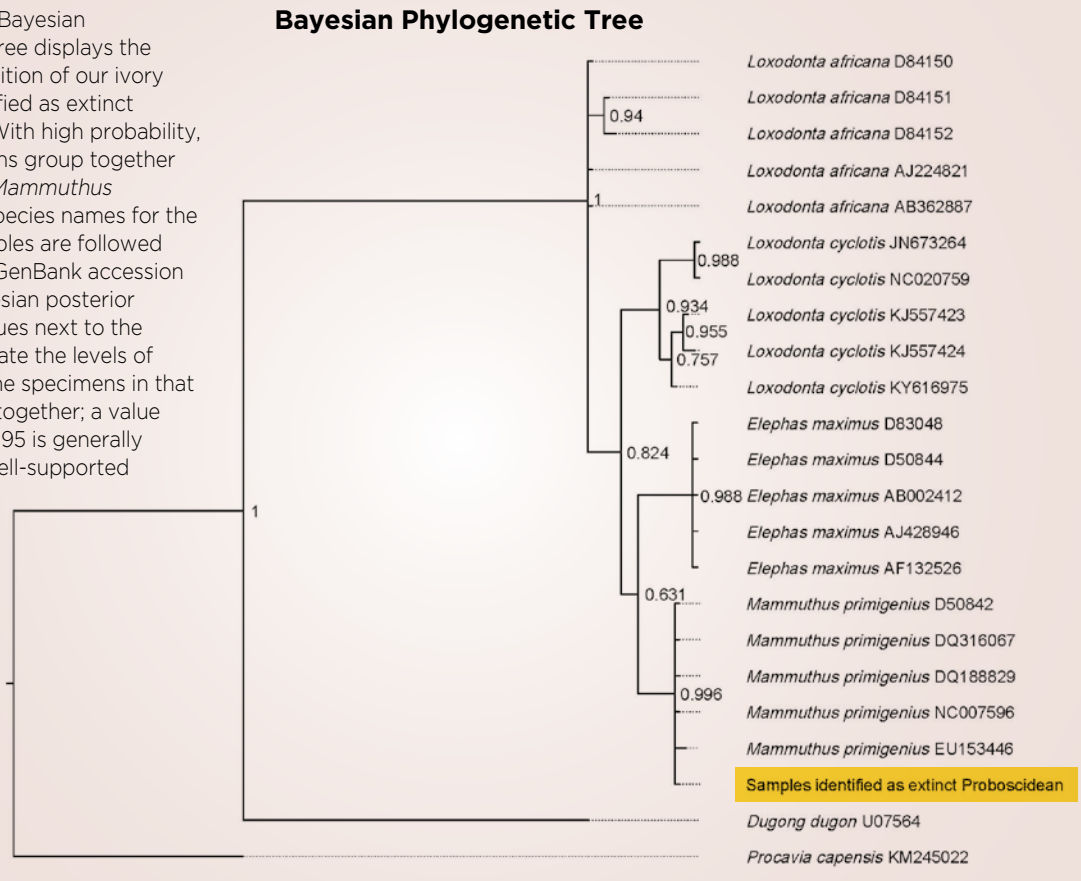

Figure 9: This Bayesian phylogenetic tree displays the taxonomic position of our ivory samples identified as extinct Proboscidea. With high probability, these specimens group together with those of *Mammuthus primigenius*. Species names for the reference samples are followed by their NCBI GenBank accession numbers. Bayesian posterior probability values next to the branches indicate the levels of support that the specimens in that branch group together; a value greater than 0.95 is generally accepted as well-supported clustering.

is a diagram representing evolutionary relationships among organisms. The included species are found at the tips of lines, referred to as tree branches. The pattern in which these branches connect represents how the species evolved from different common ancestors; a node represents a divergence event. In our phylogenetic tree, the identical DNA sequences obtained from nine of our tested samples grouped together, with high probability, with sequences of *Mammuthus primigenius*.

Combining the Results of the Morphological, Gemmological and Genetic Methods

By combining the results of all the analyses we conducted, we were able to determine the origin of all but two of the 21 samples (Table IV). Thirteen specimens were attributed to extinct Proboscideans (*Mammuthus* sp.). Five of these were identified by their morphological features (Schreger angles) and nine as a result of DNA analysis (different beads in sample no. 13 were identified by both techniques).

DNA analysis could not be used to specify the exact species of origin of four samples exhibiting inconclusive Schreger angles because their DNA extract consisted of a mixture of species. These samples were therefore identified as simply 'Proboscidean' since their extinct or extant origin could not be determined. Although the major component shown by genetic testing was ascribed to *Homo sapiens*, a human origin was ruled out due to the observed Schreger lines, so the presence of human DNA is considered contamination. Surprisingly, one of

Table IV: Taxonomic identification of the samples based on the methods used in this case study.

Sample no.	Taxonomic identification based on morphological analysis	Taxonomic identification based on DNA analysis	FTIR analysis	Taxonomic identification, considering results from all analyses
1	Proboscidea	Extinct Proboscidea	Carbonated hydroxyapatite	Extinct Proboscidea
2	Proboscidea	Mixture	Carbonated hydroxyapatite	Proboscidea
3	Proboscidea	Extinct Proboscidea	Carbonated hydroxyapatite	Extinct Proboscidea
4	Proboscidea	Extinct Proboscidea	Carbonated hydroxyapatite	Extinct Proboscidea
5	Proboscidea	Extinct Proboscidea	Carbonated hydroxyapatite	Extinct Proboscidea
6	Proboscidea	Extinct Proboscidea	Carbonated hydroxyapatite	Extinct Proboscidea
7	Extinct Proboscidea	Not performed	Carbonated hydroxyapatite	Extinct Proboscidea
8	Proboscidea	Mixture	Carbonated hydroxyapatite	Proboscidea
9	Extinct Proboscidea	Not performed	Carbonated hydroxyapatite	Extinct Proboscidea
10	Proboscidea	Mixture	Carbonated hydroxyapatite	Proboscidea
11	Not possible	Not conclusive	Carbonated hydroxyapatite	Not possible
12	Extinct Proboscidea	Not performed	Carbonated hydroxyapatite	Extinct Proboscidea
13	Extinct Proboscidea	Extinct Proboscidea	Carbonated hydroxyapatite	Extinct Proboscidea
14	Proboscidea	Extinct Proboscidea	Carbonated hydroxyapatite	Extinct Proboscidea
15	Not possible	*Bos* sp.	Carbonated hydroxyapatite	*Bos* sp.
16	Proboscidea	Extinct Proboscidea	Carbonated hydroxyapatite	Extinct Proboscidea
17	Not possible	Mixture	Carbonated hydroxyapatite	Not possible
18	Proboscidea	*Homo sapiens*	Carbonated hydroxyapatite	Proboscidea
19	Imitation	Not performed	Ivory imitation	Ivory imitation (artificial resin)
20	Not possible	Extinct Proboscidea	Carbonated hydroxyapatite	Extinct Proboscidea
21	Extinct Proboscidea	Not performed	Carbonated hydroxyapatite	Extinct Proboscidea

these specimens (no. 10) had a minor component attributed to the species *Gallus gallus*, but again because of the observed Schreger lines we know this sample did not originate from a chicken. A possible source of contamination could be residual chicken grease used to polish the specimen during manufacturing.

One sample originated from the genus *Bos* (no. 15; cattle bone) according to DNA analysis, and another (no. 19) was conclusively identified as an imitation of ivory made of artificial resin based on microscopic and FTIR analyses. Finally, two specimens (nos. 11 and 17) did not exhibit any Schreger angles, nor any other morphological characteristics indicative for ivory. DNA analysis of these items was also not successful—one sample exhibited too little or too degraded DNA, and the DNA extract of the other consisted of a mixture—so their taxonomic identification was not possible.

CONCLUSIONS

Various types of ivory may be encountered by gemmologists as *objets d'art*, jewellery and other items (e.g. Figures 1 and 10). This case study shows the challenges and limitations of distinguishing between these gem materials. To identify the nature (e.g. ivory or imitation) and species of 'ivory' samples, a combined approach using multiple techniques (in this study, morphological, gemmological and genetic) can be helpful in many instances. For this case study, determination began with morphological analysis (macroscopic and microscopic), which is the most readily available testing method. Samples not displaying orientable Schreger lines were tested further using DNA analysis. Techniques available in well-equipped gemmological laboratories (FTIR and LA-ICP-TOF-MS) were applied to further characterise

Figure 10: The carved mammoth-ivory leaves in these gold earrings are accented by diamonds and accompanied by ~2.4 ct of pink sapphires. Courtesy of Paul Farmer Goldsmith, Vail, Colorado, USA; photo by Jeff Scovil.

and document a selection of the samples, but they were not useful for identifying whether a specimen was from an extinct or extant Proboscidean species. Importantly for gemmologists, the presence of a cattle bone sample that had FTIR features similar to those of ivory shows the importance of integrating DNA analysis into origin determination when Schreger lines are not clearly visible or measurable.

Jacob *et al.* (2008) showed that the distribution of chemical elements in tusks is heterogeneous. They also proposed that isotopic rather than trace-element analysis might be more suitable for identifying the geographic source region of ivory species, but this method is outside the scope of this study. The portion of the tusk being analysed should be taken into account when carrying out trace-element and isotopic analysis of ivory specimens; if the CDJ is not present, then establishing a consistent sampling position is not possible. Furthermore, the degree of weathering (and presence of associated elements) in fossilised ivory samples, which can be 10,000 years or older, is a considerable factor to take into account. A larger reference database would be needed before attempting to use trace elements, and more specifically ultra-trace elements (e.g. REEs), to identify different ivory species.

Although the ivory trade has changed due to more stringent international regulations, material continues to be misrepresented on the market, and research such as outlined here is important to support elephant conservation work worldwide. Making techniques available to conclusively identify ivory species can help limit fraud, as in cases where poached elephant ivory is falsely declared as mammoth ivory. During an August 2019 CITES conference in Switzerland, a proposal was made (although ultimately retracted) to include mammoth ivory in CITES appendices. The ongoing interest in differentiating between extinct vs. extant ivory demonstrates the need for the reliable identification of ivory in the trade.

REFERENCES

Baker, B.W, Jacobs, R.L., Mann, M.-J., Espinoza, E.O. & Grein, G. 2020. *Identification Guide for Ivory and Ivory Substitutes*, 4th edn. CITES Secretariat, Geneva, Switzerland and World Wildlife Fund, Washington DC, USA, 108 pp., https://wwfeu.awsassets.panda.org/downloads/r8_ivoryguide_07162020_low_res.pdf.

Basilyan, A.E., Anisimov, M.A., Nikolskiy, P.A. & Pitulko, V.V. 2011. Wooly mammoth mass accumulation next to the Paleolithic Yana RHS site, Arctic Siberia: Its geology, age, and relation to past human activity. *Journal of Archaeological Science*, **38**(9), 2461–2474, https://doi.org/10.1016/j.jas.2011.05.017.

Brown, P.W. & Constantz, B. 1994. *Hydroxyapatite and Related Materials*. CRC Press, Boca Raton, Florida, USA, 368 pp., https://doi.org/10.1201/9780203751367.

Brunnermeier, M.J., Schmied, S.A.K., Müller-Boge, M. & Schupfner, R. 2012. Dating of ivory from 20th century by determination of ^{14}C by the direct absorption method. *Applied Radiation and Isotopes*, **70**(8), 1595–1602, https://doi.org/10.1016/j.apradiso.2011.10.006.

Budowle, B., Churchill, J.D. & King, J.L. 2016. The next state-of-the-art forensic genetics technology: Massively parallel sequencing. *In*: Amorim, A. & Budowle, B. (eds) *Handbook of Forensic Genetics: Biodiversity and Heredity in Civil and Criminal Investigation*. World Scientific, London, 249–291, https://doi.org/10.1142/9781786340788_0013.

Campbell Pedersen, M. 2015. *Ivory*. Robert Hale Ltd, London, 240 pp.

Cartier, L.E., Krzemnicki, M.S., Lendvay, B. & Meyer, J.B. 2018. DNA fingerprinting of pearls, corals and ivory: A brief review of applications in gemmology. *Journal of Gemmology*, **36**(2), 152–160, http://doi.org/10.15506/jog.2018.36.2.152.

Cerling, T.E., Barnette, J.E., Chesson, L.A., Douglas-Hamilton, I., Gobush, K.S., Uno, K.T., Wasser, S.K. & Xu, X. 2016. Radiocarbon dating of seized ivory confirms rapid decline in African elephant populations and provides insight into illegal trade. *Proceedings of the National Academy of Sciences*, **113**(47), 13330–13335, https://doi.org/10.1073/pnas.1614938113.

Chang, M.C. & Tanaka, J. 2002. FT-IR study for hydroxyapatite/collagen nanocomposite cross-linked by glutaraldehyde. *Biomaterials*, **23**(24), 4811–4818, https://doi.org/10.1016/S0142-9612(02)00232-6.

Chappard, C., André, G., Daudon, M. & Bazin, D. 2016. Analysis of hydroxyapatite crystallites in subchondral bone by Fourier transform infrared spectroscopy and powder neutron diffraction methods. *Comptes Rendus Chimie*, **19**(11–12), 1625–1630, https://doi.org/10.1016/j.crci.2015.03.015.

Conte, J., Potoczniak, M.J., Mower, C. & Tobe, S.S. 2019. ELEquant: A developmental framework and validation of forensic and conservation real-time PCR assays. *Molecular Biology Reports*, **46**(2), 2093–2100, https://doi.org/10.1007/s11033-019-04660-7.

Cucina, A., Dudgeon, J. & Neff, H. 2007. Methodological strategy for the analysis of human dental enamel by LA-ICP-MS. *Journal of Archaeological Science*, **34**(11), 1884–1888, https://doi.org/10.1016/j.jas.2007.01.004.

Edgar, R.C. 2013. UPARSE: Highly accurate OTU sequences from microbial amplicon reads. *Nature Methods*, **10**(10), 996–998, https://doi.org/10.1038/nmeth.2604.

Edgar, R.C. & Flyvbjerg, H. 2015. Error filtering, pair assembly and error correction for next-generation sequencing reads. *Bioinformatics*, **31**(21), 3476–3482, https://doi.org/10.1093/bioinformatics/btv401.

Edwards, H.G.M. & Farwell, D.W. 1995. Ivory and simulated ivory artefacts: Fourier transform Raman diagnostic study. *Spectrochimica Acta Part A: Molecular and Biomolecular Spectroscopy*, **51**(12), 2073–2081, https://doi.org/10.1016/0584-8539(95)01455-3.

Edwards, H.G.M., Hassan, N.F.N. & Arya, N. 2006. Evaluation of Raman spectroscopy and application of chemometric methods for the differentiation of contemporary ivory specimens I: Elephant and mammalian species. *Journal of Raman Spectroscopy*, **37**(1–3), 353–360, https://doi.org/10.1002/jrs.1458.

Espinoza, E.O. & Mann, M.-J. 1993. The history and significance of the Schreger pattern in Proboscidean ivory characterization. *Journal of the American Institute for Conservation*, **32**(3), 241–248, https://doi.org/10.1179/019713693806124866.

Espinoza, E.O. & Mann, M.-J. 2000. *Identification Guide for Ivory and Ivory Substitutes*, 3rd edn. Ivory Identification Inc., Richmond, Virginia, USA, 33 pp.

Grunenwald, A., Keyser, C., Sautereau, A.M., Crubézy, E., Ludes, B. & Drouet, C. 2014. Revisiting carbonate quantification in apatite (bio)minerals: A validated FTIR methodology. *Journal of Archaeological Science*, **49**, 134–141, https://doi.org/10.1016/j.jas.2014.05.004.

Gupta, S.K., Thangaraj, K. & Singh, L. 2011. Identification of the source of ivory idol by DNA analysis. *Journal of Forensic Sciences*, **56**(5), 1343–1345, https://doi.org/10.1111/j.1556-4029.2011.01750.x.

Harris, L., Gore, M. & Mills, M. 2019. Compliance with ivory trade regulations in the United Kingdom among traders. *Conservation Biology*, **33**(4), 906–916, https://doi.org/10.1111/cobi.13277.

Hassan, M.N., Mahmoud, M.M., El-Fattah, A.A. & Kandil, S. 2016. Microwave-assisted preparation of nano-hydroxyapatite for bone substitutes. *Ceramics International*, **42**(3), 3725–3744, https://doi.org/10.1016/j.ceramint.2015.11.044.

Jacob, D.E., Stracke, A., Wiegand, B. & Dindorf, W. 2008. Tracing ivory by its chemical and isotopic composition. *In*: Roth, J. & Bortolaso, G. (eds) *Elfenbein und Artenschutz. INCENTIVS – Tagungsbeiträge der Jahre (2004 - 2007)/Ivory and Species Conservation. Proceedings of INCENTIVS – Meetings (2004 - 2007)*. Bundesamt für Naturschutz, Bonn, Germany, **228**, 93–99, www.bfn.de/fileadmin/BfN/service/Dokumente/skripten/skript228.pdf.

Khoshhesab, Z.M. 2012. Reflectance IR spectroscopy. *In*: Theophile, T. (ed) *Infrared Spectroscopy – Materials Science, Engineering and Technology*. IntechOpen, London, 233–244, https://doi.org/10.5772/37180.

Kitpipit, T., Penchart, K., Ouithavon, K., Satasook, C., Linacre, A. & Thanakiatkrai, P. 2016. A novel real time PCR assay using melt curve analysis for ivory identification. *Forensic Science International*, **267**, 210–217, https://doi.org/10.1016/j.forsciint.2016.08.037.

Kitpipit, T., Thongjued, K., Penchart, K., Ouithavon, K. & Chotigeat, W. 2017. Mini-SNaPshot multiplex assays authenticate elephant ivory and simultaneously identify the species origin. *Forensic Science International: Genetics*, **27**, 106–115, https://doi.org/10.1016/j.fsigen.2016.12.007.

Kohn, M.J., Schoeninger, M.J. & Barker, W.W. 1999. Altered states: Effects of diagenesis on fossil tooth chemistry. *Geochimica et Cosmochimica Acta*, **63**(18), 2737–2747, https://doi.org/10.1016/s0016-7037(99)00208-2.

Lee, K.M., Appleton, J., Cooke, M., Keenan, F. & Sawicka-Kapusta, K. 1999. Use of laser ablation inductively coupled plasma mass spectrometry to provide element versus time profiles in teeth. *Analytica Chimica Acta*, **395**(1–2), 179–185, https://doi.org/10.1016/s0003-2670(99)00319-0.

Lee, E., Lee, Y., Moon, S., Kim, N., Kim, S., Yang, M., Choi, D. & Han, M. 2013. The identification of elephant ivory evidences of illegal trade with mitochondrial cytochrome b gene and hypervariable D-loop region. *Journal of Forensic and Legal Medicine*, **20**(3), 174–178, https://doi.org/10.1016/j.jflm.2012.06.014.

Lendvay, B., Cartier, L.E., Gysi, M., Meyer, J.B., Krzemnicki, M.S., Kratzer, A. & Morf, N.V. 2020. DNA fingerprinting: An effective tool for taxonomic identification of precious corals in jewelry. *Scientific Reports*, **10**, article 8287 (12 pp.), https://doi.org/10.1038/s41598-020-64582-4.

Limbeck, A., Galler, P., Bonta, M., Bauer, G., Nischkauer, W. & Vanhaecke, F. 2015. Recent advances in quantitative LA-ICP-MS analysis: Challenges and solutions in the life sciences and environmental chemistry. *Analytical and Bioanalytical Chemistry*, **407**(22), 6593–6617, https://doi.org/10.1007/s00216-015-8858-0.

Morf, N.V., Wood, K.L., Köppel, R., Felderer, N., Daniels, M., Tenger, B. & Kratzer, A. 2013. A multiplex PCR method to identify bushmeat species in wildlife forensics. *Forensic Science International: Genetics Supplement Series*, **4**(1), e202–e203, https://doi.org/10.1016/j.fsigss.2013.10.104.

Ngatia, J.N., Lan, T.M., Ma, Y., Dinh, T.D., Wang, Z., Dahmer, T.D. & Chun Xu, Y. 2019. Distinguishing extant elephants ivory from mammoth ivory using a short sequence of cytochrome b gene. *Scientific Reports*, **9**, article 18863 (12 pp.), https://doi.org/10.1038/s41598-019-55094-x.

Nikolskiy, P.A., Sulerzhitsky, L.D. & Pitulko, V.V. 2011. Last straw versus Blitzkrieg overkill: Climate-driven changes in the Arctic Siberian mammoth population and the Late Pleistocene extinction problem. *Quaternary Science Reviews*, **30**(17–18), 2309–2328.

O'Connor, S., Edwards, H.G.M. & Ali, E. 2011. An interim investigation of the potential of vibrational spectroscopy for the dating of cultural objects in ivory. *ArcheoSciences*, **35**, 159–165, https://doi.org/10.4000/archeosciences.3091.

Ronquist, F., Teslenko, M., van der Mark, P., Ayres, D.L., Darling, A., Höhna, S., Larget, B., Liu, L. *et al*. 2012. MrBayes 3.2: Efficient Bayesian phylogenetic inference and model choice across a large model space. *Systematic Biology*, **61**(3), 539–542, http://doi.org/10.1093/sysbio/sys029.

Schmied, S.A.K., Brunnermeier, M.J., Schupfner, R. & Wolfbeis, O.S. 2012. Dating ivory by determination of ^{14}C, ^{90}Sr and $^{228/232}Th$. *Forensic Science International*, **221**(1–3), 5–10, https://doi.org/10.1016/j.forsciint.2012.02.017.

Schreger, B.N.G. 1800. Beitrag zur Geschichte der Zähne. *Beiträge für die Zergliederungkunst*, **1**, 1–7.

Shimoyama, M., Morimoto, S. & Ozaki, Y. 2004. Non-destructive analysis of the two subspecies of African elephants, mammoth, hippopotamus, and sperm whale ivories by visible and short-wave near infrared spectroscopy and chemometrics. *Analyst*, **129**(6), 559–563, https://doi.org/10.1039/b401003e.

Singh, R.R., Goyal, S.P., Khanna, P.P., Mukherjee, P.K. & Sukumar, R. 2006. Using morphometric and analytical techniques to characterize elephant ivory. *Forensic Science International*, **162**(1–3), 144–151, https://doi.org/10.1016/j.forsciint.2006.06.028.

Tobe, S.S. & Linacre, A. 2010. DNA typing in wildlife crime: Recent developments in species identification. *Forensic Science, Medicine, and Pathology*, **6**(3), 195–206, https://doi.org/10.1007/s12024-010-9168-7.

Trapani, J. & Fisher, D.C. 2003. Discriminating Proboscidean taxa using features of the Schreger pattern in tusk dentin. *Journal of Archaeological Science*, **30**(4), 429–438, https://doi.org/10.1006/jasc.2002.0852.

United Nations Office on Drugs and Crime (UNODC) 2014. *Guidelines on Methods and Procedures for Ivory Sampling and Laboratory Analysis*. United Nations, Vienna, Austria, 119 pp., www.unodc.org/res/cld/bibliography/guidelines-on-methods-and-procedures-for-ivory-sampling-and-laboratory-analysis_html/Guidelines_Ivory.pdf.

van der Merwe, N.J., Lee-Thorp, J.A., Thackeray, J.F., Hall-Martin, A., Kruger, F.J., Coetzee, H., Bell, R.H.V. & Lindeque, M. 1990. Source-area determination of elephant ivory by isotopic analysis. *Nature*, **346**(6286), 744–746, https://doi.org/10.1038/346744a0.

Vigne, L. & Martin, E. 2014. *China Faces a Conservation Challenge: The Expanding Elephant and Mammoth Ivory Trade in Beijing and Shanghai*. Save the Elephants and The Aspinall Foundation, Nairobi, Kenya and Lympne, Nr Hythe, Kent, 89 pp., http://savetheelephants.org/wp-content/uploads/2014/12/2014_ChinaConservationChallenge.pdf.

Wang, H.A.O., Krzemnicki, M.S., Chalain, J.-P., Lefèvre, P., Zhou, W. & Cartier, L. 2016. Simultaneous high sensitivity trace-element and isotopic analysis of gemstones using laser ablation inductively coupled plasma time-of-flight mass spectrometry. *Journal of Gemmology*, **35**(3), 212–223, https://doi.org/10.15506/JoG.2016.35.3.212.

Wozney, K.M. & Wilson, P.J. 2012. Real-time PCR detection and quantification of elephantid DNA: Species identification for highly processed samples associated with the ivory trade. *Forensic Science International*, **219**(1–3), 106–112, https://doi.org/10.1016/j.forsciint.2011.12.006.

Yin, Z., Zhang, P., Chen, Q., Luo, Q., Zheng, C. & Li, Y. 2013. A comparison of modern and fossil ivories using multiple techniques. *Gems & Gemology*, **49**(1), 16–27, https://doi.org/10.5741/gems.49.1.16.

Ziegler, S., Merker, S., Streit, B., Boner, M. & Jacob, D.E. 2016. Towards understanding isotope variability in elephant ivory to establish isotopic profiling and source-area determination. *Biological Conservation*, **197**, 154–163, https://doi.org/10.1016/j.biocon.2016.03.008.

The Authors

Dr Laurent E. Cartier FGA
Swiss Gemmological Institute SSEF, Aeschengraben 26, 4051 Basel, Switzerland, and Institute of Earth Sciences, University of Lausanne, 1015 Lausanne, Switzerland
Email: laurent.cartier@ssef.ch

Dr Michael S. Krzemnicki FGA
Swiss Gemmological Institute SSEF, Aeschengraben 26, 4051 Basel, Switzerland

Mario Gysi, Dr Bertalan Lendvay and Nadja V. Morf
Zurich Institute of Forensic Medicine, University of Zurich, Winterthurerstrasse 190/52, 8057 Zurich, Switzerland

Acknowledgements

We thank Karl Ammann for providing the samples for this study and the OAK Foundation for funding part of this research. We also thank Gina Brombach, Judith Braun and Dr Hao Wang of SSEF for their help with FTIR and LA-ICP-TOF-MS analyses, and Vito Lanzafame of SSEF for specimen photos. Dr Ed Espinoza (U.S. Fish & Wildlife Service Forensics Laboratory, Ashland, Oregon) is thanked for kindly providing Figure 2.